SLAC-PUB-3345
May 1984
(N)

# THE EP OPTION AT THE SSC*

CHARLES Y. PRESCOTT
*Stanford Linear Accelerator Center*
*Stanford University, Stanford, California 94305*

**Abstract**

The possibilities for colliding electrons with the 20 TeV proton beams of the SSC is considered. Kinematics of ep colliding beams is reviewed. Energies that may be possible and interesting are suggested, and detector problems associated with the highly imbalanced collisions are briefly considered.

## 1. Introduction

The purpose of this talk is to set the scale of an ep alternative to a fixed target program at the SSC. This report is the first look at ep physics using the 20 TeV protons planned for the SSC. The work has just begun and hopefully will continue in the next few months leading to a well defined set of ep parameters as an option for the physics programs of the SSC. The basic objective of this report is to define those opportunities and parameters, estimate the effort and associated costs needed to achieve an exciting physics program, and provide a basis for comparison with other options. The best example for an alternative to an ep project would be a fixed target facility having muon and neutrino beams available. Comparison of physics capabilities and costs is essential before a decision on which direction to proceed, or indeed whether to proceed, can be made. Since the study has been underway for only a few months, many topics are in rather preliminary state, and will need considerable further work. Many of the physics issues have been discussed in other places, including the SNOWMASS 82 report and several HERA reports, for example. Extrapolation of these ideas to SSC energies may be straightforward, but new calculations must be done in most cases. The energies that can reached, and the new processes that may emerge lie well beyond our present experience. An ep facility at the SSC of moderate cost and effort would certainly broaden and balance the program, and may well provide the greatest excitement at the frontiers of particle physics.

## 2. Physics Opportunities

(a) Recent History

The recent past of particle physics is dominated by deep inelastic lepton-nucleon scattering. Some of the most significant progressive steps were begun in the inelastic scattering experiments of the early 1970's and continuing up to present times. The early eN experiments observed the parton-like structure of the nucleon through scaling behavior of the inelastic structure functions. Evidence that these partons were fractionally charged spin 1/2 quarks was seen in measurements of neutron to proton ratios for the structure functions and in the values of $R = \sigma_L/\sigma_T$. Neutrino inelastic scattering showed these features as well, and the ratios of $\mu$N and eN structure functions lent strong support to the quark model. Precise measurements of quark and anti-quark composition in nucleons became possible with neutrino beams.

The first hint that gluons are present in nuclei was seen in the early eN measurements. The momentum sum rules showed that hadronic constituents which do not interact with an electron probe exist in the nucleon. Further evidence for gluons emerged in the violation of scaling behavior as energies and $Q^2$'s increased, confirming predictions that structure functions would soften as $Q^2$ values increased. Detailed studies of the structure functions from eN and $\nu$N inelastic scattering yielded the first measurements of QCD parameters, and clearly indicated a preference for a spin 1 gluon over spin 0.

Electroweak effects were first seen in $\nu$N scattering with the discovery of neutral currents at CERN. The best measurements of the electroweak parameter $\sin^2\theta_W$ comes from $\nu$N inelastic scattering. Electromagnetic-weak interference effects predicted by the electroweak theory were first clearly seen and studied in eN and $\mu$N inelastic scattering.

This recent history of success in deep inelastic scattering cannot be ignored. The lesson in this record is obvious. Inelastic scattering has been an enormously rich field and will continue to be so.

(b) Structure Functions

The present knowledge of nucleon structure at high $Q^2$ is illustrated in Fig. 1. These results are a collection of data for $\mu$N and $\nu$N scattering. These data show a clear slope in $F_2$, at fixed $x$, as $Q^2$ increases. For low values of $x$, the slope is positive. For high values, it is negative. Present data extend out to $Q^2 \approx 200$ (GeV/c)$^2$. Extension of these data by more than two orders-of-magnitude is possible at the SSC. From such measurements will come further tests of QCD predictions over the much extended kinematical range. Deviations from QCD-like behavior will occur when new processes begin to open

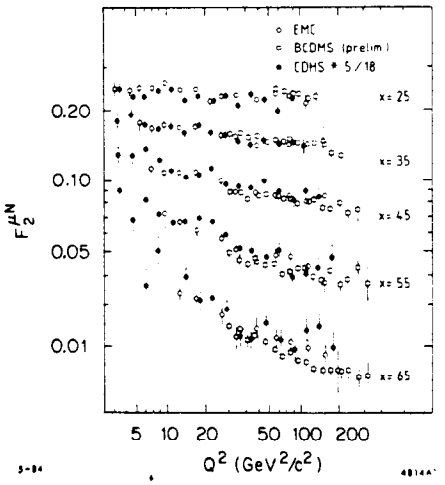


Fig. 1. The present status of $F_2$ is illustrated with data from three experiments (from F. Eisele, Proceedings of the 21st Int. Conference on High Energy Physics, Paris 1982). The data which extend to $Q^2 \approx 200(GeV/c)^2$ are shown for several values of $x$.

* Work supported by the Department of Energy, contract DE-AC03-76SF00515

Presented at the Meeting of the PSSC Steering Committee, PSSC Task Force Groups and Fixed Target Summary, Woodland, Texas, January 29-30, 1984

up. Some of these processes have large effects and would easily be observed; others have small effects and may be difficult to separate out. Whatever occurs, the measurements of nucleon structure in the extended kinematical range will be enormously important to our understanding of high energy processes.

(c) Conventional Processes at Higher Energies

Three familiar processes which contribute to ep scattering are shown in Fig. 2. These include an intermediate virtual photon scattering from a quark or anti-quark, a virtual $Z^0$ exchange, a charged W exchange with an outgoing neutrino, and a virtual photon-constituent gluon interaction.

The processes shown in Fig. 2 will have distinctly differing behaviors in a detector. The neutral current events will have an isolated electron, with transverse momentum-energy balance given by a jet of hadrons opposite to the electron. Charged current events will be distinguished by single jets not accompanied by an electron on the opposite side. The photon-gluon fusion process shown in Fig. 2 will occur at predominantly low-$Q^2$ kinematics, and will have extra hadrons and jets in the event; this is the "two-photon" equivalent to the similar process studied in $e^+e^-$ interactions. Each of the above processes will be interesting to study in the high energy regime.

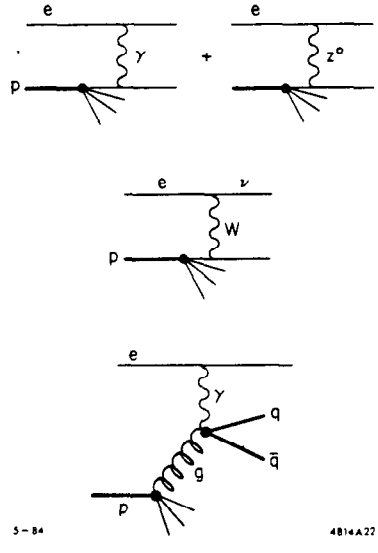


Fig. 2. Three conventional processes which contribute to events in ep scattering.

(d) Polarization

The cross sections for these processes in Figs. 2(a) and 2(b) are strongly polarization dependent. The electrons beams can be polarized through the natural mechanism associated with quantum fluctuations in magnetic fields. This process, first discussed by Sokolov and Ternov has been observed and studied in present storage rings, and is expected to exist in HERA. It may be possible to polarize e beams for an SSC facility, but only in designs for the e-ring having energies below about 40 GeV. Circular rings above this value are predicted to have little useful polarization.

The conventional use of polarization is for the detailed study of neutral current and charged current processes. The polarization asymmetries are expected to be large. For charged currents, the predictions of the standard electroweak phenomenology are simple; $e_L^-$ processes are allowed, but $e_R^-$ processes are forbidden by the V–A coupling. A search for right-handed currents is of considerable importance, and could readily be done using polarized e beams in ep scattering. High polarizations help but are not essential to make this search. Deviations from the purely V–A nature of the process can be measured out to $Q^2 \rightarrow 10^5$ $(GeV/c)^2$ and sensitivity to $W_R$ masses up to 1 TeV is possible by this technique.

## 3. Kinematics of ep Interactions at the SSC

(a) Kinematic Variables

The kinematics of deep inelastic scattering has always been an integral part of all discussions of the field. Knowledge of the variables and the notation is generally assumed to be well understood. In the case of ep collisions at the SSC, where the proton motion so strongly dominates the event kinematics and distorts the angles and momenta compared to the more familiar fixed target studies, a brief review of inelastic scattering seems appropriate.

The basic ideas of inelastic scattering are illustrated in Fig. 3. A massless incident lepton (here an electron) scatters elastically from a massless incident parton, shown in the center-of-mass of that event. In a diagram where $p_\perp$ and $p_\parallel$ are plotted vertically and horizontally , respectively, the lepton and parton scatter back-to-back at various cms angles, with equal outgoing momenta. The momentum vectors lie on a circle about the origin. In the lab frame, these momenta are transformed, to the left or to the right, depending on tne angles and momenta involved. The circle transforms into an ellipse. If the electron has energy $E_e$, the incoming proton has energy $E_p$, the parton has fractional momentum $xE_p$, and $\theta_e$ is the angle of the scattered electron relative to its incoming direction, the usual kinematic variables are:

$$s = 4E_eE_p$$

$$Q^2 = 2E_eE'_e(1 - cos\theta_e)$$

$$\nu = P_p \cdot q/M_p$$

$$y = \nu/\nu_{max} = 2P_p \cdot q/s$$

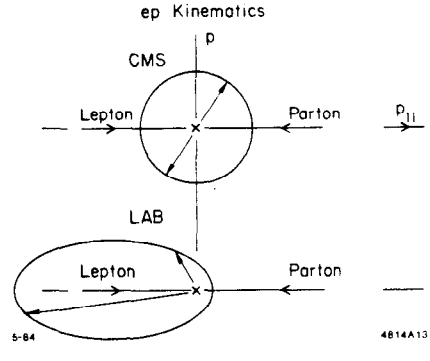


Fig. 3. The kinematics of ep scattering in a $p_\parallel$ versus $p_\perp$ diagram for (a) In the lepton-parton cms, and (b) In the lab.

$$x = Q^2/2P_p \cdot q = Q^2/sy$$

$$v = Q^2/Q^2_{max}$$

From these definitions and momentum-energy conservation the following relations result:

$$1/E'_e = \frac{xE_p + E_e}{2xE_eE_p}\left[1 + \frac{xE_p - E_e}{xE_p + E_e}cos\theta_e\right]$$

$$1/E'_{jet} = \frac{xE_p + E_e}{2xE_eE_p}\left[1 + \frac{xE_p - E_e}{xE_p + E_e}cos\theta_{jet}\right]$$

$$Q^2_{max} = 4xE_pE_e \text{ at } \theta_e = \pi$$

$$P_{\perp max} = \sqrt{E_eE_p}$$

$$x_{min}(\text{at fixed } Q^2) = Q^2/4E_eE_p$$

where $cos\theta_e = \hat{p}_e \cdot \hat{p}'_e$ and $cos\theta_{jet} = \hat{p}_p \cdot \hat{p}_{jet}$

Figure 4 shows the customary ellipse associated with ep scattering kinematics. In the $p_{\parallel}$ versus $p_{\perp}$ plot, ellipses are shown as contours for constant values of $x$ from 0 to 1.0. In Fig. 4(a), the range of variables is shown. The maximum electron energy at $\theta = 0$ is $E_e$; at $\theta = \pi/2$ it is $2E_e$. The maximum transverse momentum is $p_{\perp}(max) = \sqrt{E_eE_p}$, and the electron carries an energy $(E_e + E_p)/2$ at this point. The angle is given by $\sin\theta(max) = 2\sqrt{E_eE_p}/(E_e + E_p)$.

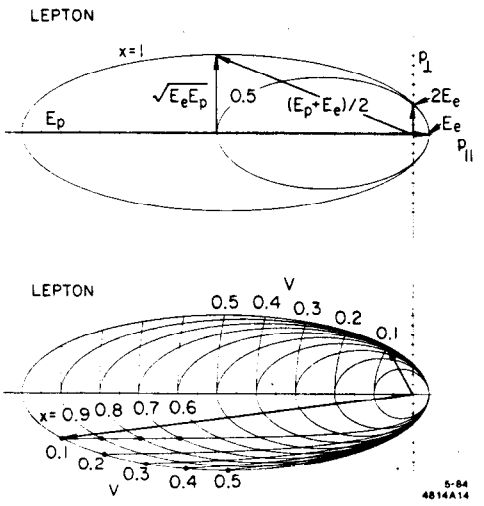


Fig. 4. (a) An envelope of ep scattering for $x = .5$ and $x = 1.0$. (b) The same as a), but for $x = .1$-1.0. Contours of $v = Q^2/Q^2_{max}$ are also shown for the lepton (the upper half) and the jet (the lower half).

On the hadronic side, the maximum energy is $E_p$ at $x = 1$ (elastic scattering). Figure 4(b) shows the same ellipses, but for 10 values of $x$. Here contours of $v = Q^2/Q^2_{max}$= constant have been added. Notice that the $Q^2$ contours for the lepton and hadron side are different. With the lower part of Fig. 4, correlations between the electron and hadron jet directions are obtained by connecting points of fixed $x$ and $Q^2$ to the origin. Angles corresponding to those $x$ and $Q^2$ values can be read off. One example is illustrated.

In reality, the SSC energy of 20 TeV leaves the kinematics highly unbalanced for all realistic electron energies. Figure 5 shows four cases considered later, namely $E_e = 5$, 15, 30, and 250 GeV, for the two values $x = .5$, and $x = 1.0$. These highly unbalanced event topologies lead to problems for detector and IR hall design.

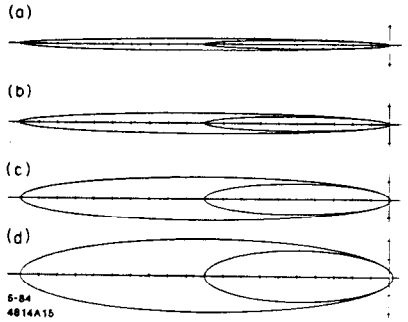


Fig. 5. Actual shapes of ep kinematics for the four energies 5, 15, 70, and 250 GeV. The ticmarks on the axes are spaced in 1 TeV intervals.

(b) Counting Rates

Counting rates are generally split into two or more categories defining different classes of physics processes. The discussions of Section 2 and the estimated cross sections for those processes can readily be converted to rates once a luminosity value is known or assumed. For the purposes of this report, a luminosity value of $L = 10^{32}$ cm$^{-2}$sec$^{-1}$ is used. This may be somewhat optimistic; HERA's design luminosity is $0.5 \times 10^{32}$ cm$^{-2}$ sec$^{-1}$, while preliminary estimates for ep at the SSC lead to similar numbers. When averaging over a calendar year to estimate total yield, an efficiency factor to account for planned shutdowns and unplanned breakdowns is common; a factor of 1/3 is reasonable. Thus given a $\sigma$= 1 picobarn, the yield of events is, for example,

$$\text{Counts} = \sigma \int L\,dt = 10^{-36} \cdot 10^{32} \cdot 3 \times 10^7 \cdot 1/3$$

$$= 1000 \text{ events/year}$$

Thus it seems possible to study processes at the fraction-of-a-picobarn level, but not at the femtobarn level.

Table I shows the counting rates for the conventional neutral current and charged current processes for the energies indicated. In this table, events are counted and binned into intervals in $x$ and $y$. The loss of events at the highest $Q^2$ is serious. The reason for the lack of events, even for the purely weak charged current process, is that the $Q^2$ values are larger than $M^2_W$ or $M^2_{Z^0}$, and propagator effects (i.e., terms that behave like $1/(Q^2 + M^2)$) are in operation at these high $Q^2$'s.

Table I. Neutral Current Events/Day at L = $10^{32}$ cm$^{-2}$ sec$^{-1}$

| $E_e$ = 30 GeV | | $x$ | | | |
|---|---|---|---|---|---|
| $E_p$ = 20 TeV | | .1 - .3 | .3 - .5 | .5 - .7 | .7 - .9 |
| | .7 - .9 | .44 | .04 | 0 | 0 |
| $y$ | .5 - .7 | 1.8 | .17 | .07 | 0 |
| | .3 - .5 | 6.0 | .58 | .07 | 0 |
| | .1 - .3 | 272 | 25 | 3.2 | .2 |

| $E_e$ = 70 GeV | | $x$ | | | |
|---|---|---|---|---|---|
| $E_p$ = 20 TeV | | .1 - .3 | .3 - .5 | .5 - .7 | .7 - .9 |
| | .7 - .9 | .19 | .02 | 0 | 0 |
| $y$ | .5 - .7 | .75 | .07 | .01 | 0 |
| | .3 - .5 | 2.6 | .24 | .03 | 0 |
| | .1 - .3 | 108 | 11 | 1.3 | .07 |

(c) Resolution

The ability to measure $x$ and $Q^2$ using conventional techniques is seriously degraded by the distorted and imbalanced kinematics presented by ep scattering at SSC energies. This problem has been studied in some detail for HERA and influences somewhat the choice of detection technologies and techniques. At the SSC, these problems are considerable and more difficult to handle.

Degraded resolution in $x$ and $Q^2$ will effect the shapes of structure functions $F_i(x, Q^2)$ through smearing. The rapidly varying functional form $F_i(x)$ expected at high $Q^2$ requires very good experimental resolution to measure properly; without it, careful measurements of the shapes of $F_i(x, Q^2)$ are in jeopardy. Figure 6 shows the expected resolution in $x$ and $Q^2$, based on calorimetric measurements for the electron (neutral current events) and for the hadronic side (both neutral current and charged current events) for specific assumptions on electron and hadron angle and energy resolutions.

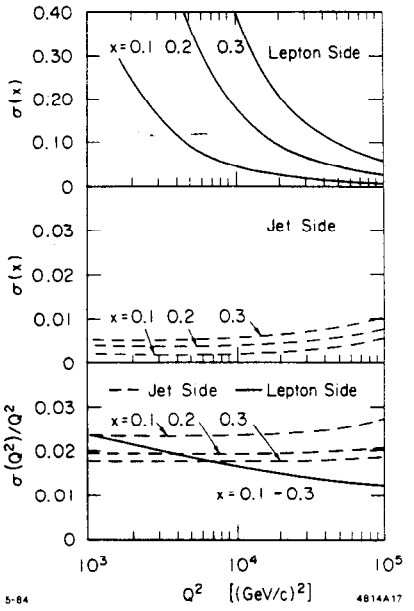


Fig. 6. Resolution in $x$ and $Q^2$ based on electron and hadron (jet) measurements for the range of $x$ and $Q^2$ shown. The electron was assumed to be measured with an energy resolution of $\sigma(E)/E = .07/\sqrt{E} + .01$ and a $\sigma(\theta) = 5$ mrad. The hadron jet was assumed to be measured with an energy resolution of $\sigma(E)/E = .7/\sqrt{E}$ and an angular resolution of 5 mrad.

## 4. Scenarios

The determination of the array of machine and experimental parameters that make reasonable sense is rather difficult. The most important of these parameters are, of course, energy and luminosity. Many of the physics goals require the highest energies and highest luminosities. The the fact that HERA already will be running and conducting experiments also sets a lower bound to the energy scale. With these constraints in mind, some possible scenarios might be:

(i) A low energy, small radius electron ring "experiment" (5 GeV electrons on 20 TeV protons)

The most inexpensive of the ep options would be a small electron ring having a low energy, say in the 5 GeV range. The extreme imbalance of energies between electron and proton would require a highly elongated distribution of instrumentation along the beam lines, and in fact may not be possible to effectively instrument. The main advantage of such a scheme lies in its low cost. Estimates of cost would be reasonably accurate, based on similarities in size to existing storage rings. Experience with these existing rings would permit optimizing performance with reasonable confidence and lowest costs. There are, however, several disadvantages. The low energy of the electron beams means that the physics goals would be similar to those of HERA. The available center-of-mass energy range is $\sqrt{s} = 2\sqrt{E_e E_p} = 632$ GeV or 2 x HERA. The interesting events may always disappear down the main ring beam pipe or go into main ring magnets where physics instrumentation cannot be located. Nevertheless, this inexpensive option might be a cheap competitor to HERA physics. The conventional facilities associated with this option would have a small tunnel and presumably one interaction hall.

(ii) A moderate energy, medium radius electron ring (15 GeV electrons on 20 TeV protons)

This alternative is a modest variation on (i) providing more energy at the expense of some more money. The center-of-mass energy available in this scheme is $\sqrt{s} = 1095$ GeV or 3.5 x HERA. Conventional construction for this option would require tunneling similar to PEP or PETRA, plus one or two interaction regions. The costs could be estimated and the performance could be planned reasonably reliably using the experiences from PEP and PETRA.

(iii) A medium energy facility (30 GeV electron on 20 TeV protons)

A highly attractive possibility that the booster tunnel could be utilized for a 30 GeV ring provides energies sufficient to open up new physics territory for a relative modest cost. The energy available in this option would be $\sqrt{s} = 1550$ GeV or 5 x HERA.

The costs would be reduced by the possibility of sharing tunnel facilities (although introducing another ring into that tunnel would certainly run up its costs). Additional expenditures for an experimental hall would be part of the costs of this option. Experience with 30 GeV operation would exist at KEK and DESY, so this ring would not be the first attempt in this energy range. However a clear disadvantage of this option lies in the constraints imposed on the booster tunnel location relative to the SSC main ring. A careful study of compatibility with SSC design requirements would be necessary before proceeding in this direction.

(iv) A high energy project (150-250 GeV electrons utilizing the SSC main ring, on 20 TeV protons)

The very high energies possible provide the best possibility for studying new physics beyond the standard electroweak phenomenology. The energies available reach up to a possible $\sqrt{s} = 4.5$ TeV or 14 x HERA. The envelope of momenta for this extreme case is shown in Fig. 5. The costs of this option are not possible to determine, but would require an extensive design study. Among the advantages of this option are the extreme energies that could be achieved and correspondingly the greatest chances for discovery. The kinematics are the best balanced of the options discussed here. The primary disadvantages are the costs, which are certainly high, the lack of experience at these energies, lack of polarization, and the interference with other SSC objectives.

## 5. Detector Problems

The choice of detector technologies and detector components for ep experimentation will be strongly influenced by details of the machine design near the interaction region. The problems of bringing electrons into collision with the proton beam will force certain compromises on location and type of detector components.

Measurement of neutral current events requires identification of the outgoing electron. Scattered electron energies range from the incident beam energy, $E_e$, at angles backward to the proton beam, up to very high energies in the direction of the proton beam. Magnetic fields combined with tracking systems have poor resolution at these energies, but electromagnetic calorimetry should work reasonably well. Resolution in $x$ and $Q^2$ are determined by the energy resolution. Coverage in e.m. calorimetry should be nearly complete to avoid confusion with charged current processes, where the outgoing lepton is an undetected neutrino.

In order to obtain resolution in $x$, the measurement of the outgoing electron alone is not sufficient. Accuracy in $x$ requires detection of the hadronic side of the process, i.e., the current jet, usually at small angles (see Fig. 6).

Hadronic calorimetry is essential for the determination of the jet parameters. In the case of charged current events, only hadronic information can be used for determination of the event kinematics. Resolution in $x$ and $Q^2$ require both good angular resolution and good energy resolution. Tracking systems may help in determination of kinematic parameters, but good calorimetry is essential.

Figure 7 shows an example of a general purpose ep detector not yet particularly optimized for any physics, but useful for illustration of some problems. The choices for this example are:

(i) Non-magnetic.

(ii) Central tracking systems surrounding the interaction point.

(iii) e.m. calorimetry surrounding most of the interaction point; beam holes forward and backward are the only missing solid angle.

(iv) Hadron calorimetry surrounding the central region, but with more emphasis in the forward region where the hadrons have higher density and energies.

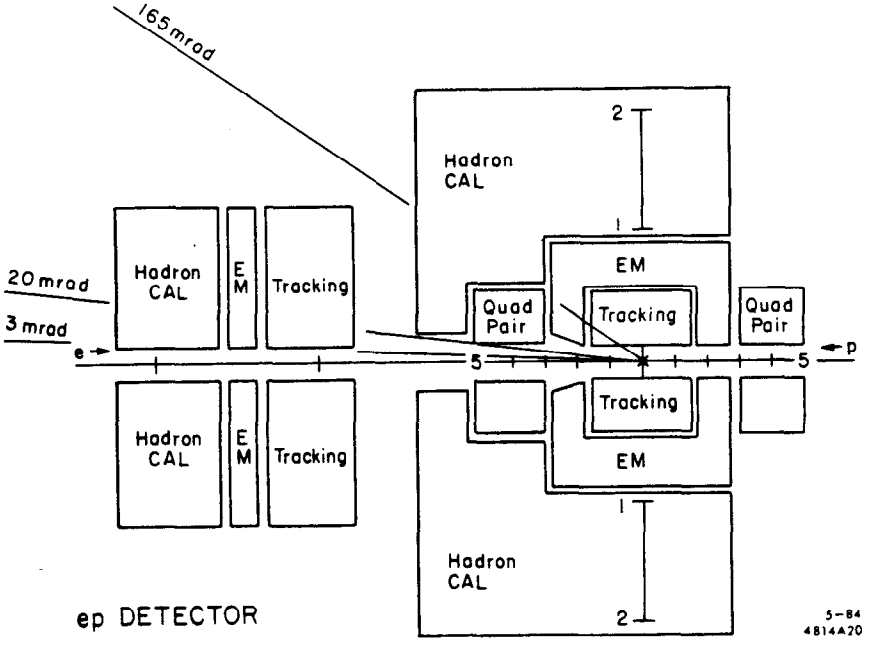


Fig. 7. A example of an ep detector, illustrating three important forward angles, 3 mrad (beam pipe), 20 mrad (quadrupole aperture) and 165 mrad (quadrupole outer edges).

(v) Quadrupoles for the electron ring imbedded within the central hadron calorimetry at one end.

(vi) Forward tracking, e. m. and hadronic calorimetry located in the forward direction of the protons.

Angles that the various components intercept in the forward direction are shown. The beam pipe is assumed to cover out to 3 mrad. The quadrupole face begins at 20 mrad and subtends solid angle out to 165 mrad. Outside of the angles the central detector is unimpeded by these components.

Figures 8(a)-8(d) show how these angles cut across the kinematic plane in $x$ and $Q^2$, for the electron beam energies of 5, 15, 70, and 250 GeV. The widely different cases all have similar problems. The quadrupoles occupy a very important part of the real estate. In all cases, hadronic jets prefer to go into the faces of these quadrupoles for a considerable portion of the kinematics of interest. The design and optimization of a general purpose detector cannot proceed in the absence of an electron ring design. The same territory that the detector needs must be occupied by components of the machine. The need for machine quadrupoles to be close to the interaction point interferes with the detector requirement for hadron calorimetry in the forward direction. An integrated design may be required, combining the functions of machine and detector into the same components. An example of this would be a novel design of a quadrupole, whereby focussing properties for the electron beam and calorimetric properties from instrumented slots in the laminations could be achieved simultaneously. Such innovative solutions to difficult technical problems may be required to make physics experiments and machine performance compatible.

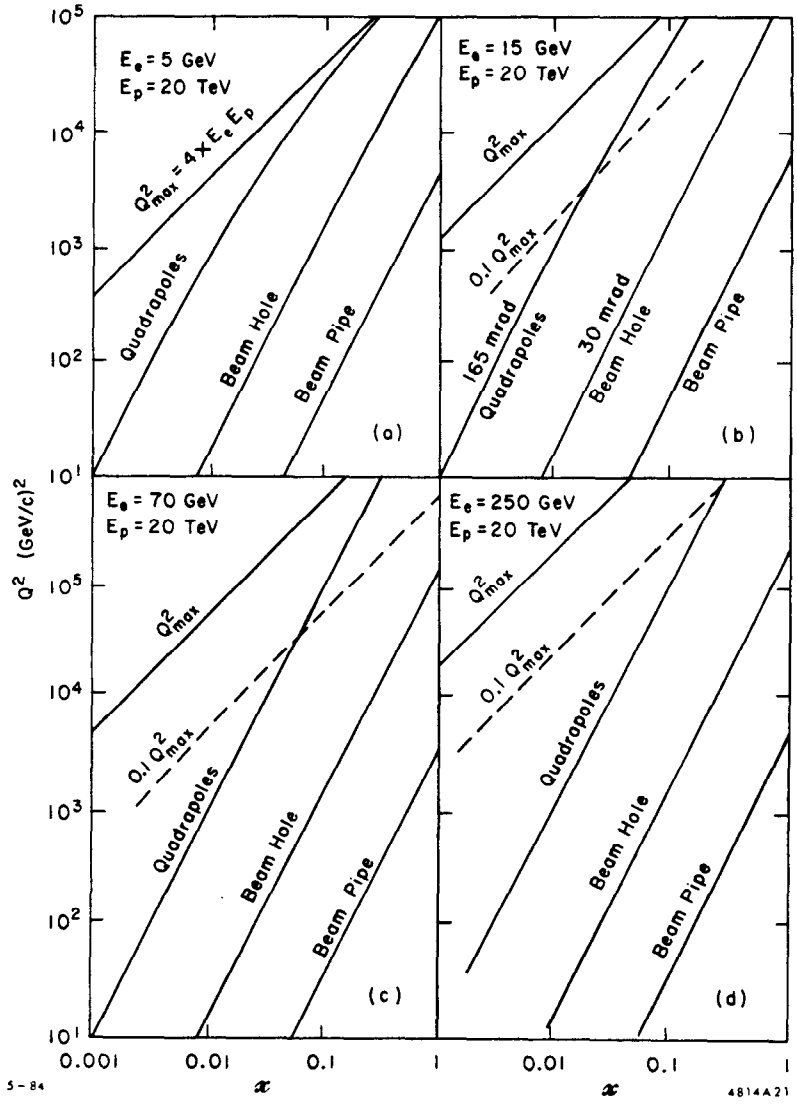


Fig. 8. Kinematic territory covered by the three polar angles of Fig. 7, for four electron energies.

## 6. Conclusions

Consideration of physics goals and opportunities show that the highest energies and luminosities are required to test the most interesting new ideas. Investigation of structure functions and electroweak processes is possible for electron energies up to 30 GeV colliding on proton beams of 20 TeV. Polarized electron beams are possible at these rings having energies up to 30 GeV, and permit detailed studies of the electroweak structure. Searches for new phenomena such as supersymmetry particles, new heavy leptons or quarks, right-handed currents, and composite structure of leptons and quarks, are possible, but are strongly enhanced by higher energies.

Kinematics of ep at the SSC are highly imbalanced, with hadronic fragments from the collisions boosted into the forward direction. Studies to optimize detectors and experimental halls for ep physics have not yet been carried out. It is apparent, however, that conflicts between machine components, particularly for the electron ring, and experimental apparatus will exist. Integration of functions in some elements, such as quadrupoles, must be considered.

An attractive idea which may significantly reduce costs for an ep facility at the SSC has the electron ring located in the booster tunnel for the main ring. This possibility could provide sufficient electron beam energy to open up new physics at modest costs. The requirement of closely located quads, combined with the highly asymmetric event topologies, indicates a need to design specialized quads which can serve as calorimeters for hadron jets in the forward direction.

Much work remains to be done. Studies of event signatures and kinematics for new physics will affect the design of a detector. Definition of an optimized ep detector is needed. Studies of techniques to calorimetrize a quadrupole would be useful. A study of IR hall size and shape is still needed. It is hoped that these studies to define the scope of an ep option for the SSC will continue at the SNOWMASS 84 workshop. The ultimate benefits of such a facility would be the balance and breadth they bring to the physics at the SSC.